ACS OMEGA

Open Access

http://pubs.acs.org/journal/acsodf

Article

Engineering GO-pAmOx: A Polyoxazoline-Functionalized Graphene Oxide Composite for Selective Removal of NSAIDs and Organic Pollutants from Water

Luca Stefanuto,* Agnese Ricci, Elisa Fardelli, Sara Del Galdo, Simone Pepi, Valerio Graziani, Luca Tortora, Claudio Rossi, Valentina Arena, Corrado Bongiorno, Emanuele Smecca, Giovanni Capellini, Barbara Capone, Daniela Tofani, and Tecla Gasperi*

Cite This: *ACS Omega* 2025, 10, 30087−30099

Read Online

ACCESS | Metrics & More | Article Recommendations | Supporting Information

ABSTRACT: Organic wastewater compounds (OWCs) employed in human activities are, nowadays, commonly detected in surface water, groundwater, and drinking water. In particular, pharmaceuticals have caused great concern because after their consumption, traces of metabolites are excreted and reach the water resources either directly or after inefficient treatment. Despite this, these compounds are not regulated in drinking water, and existing toxicity data are inadequate to assess potential risks from chronic low-dose exposure. Considering the necessity to find new efficient, reusable, and biocompatible systems to remove organic pollutants from wastewater, the adsorption process has been found to be the most effective and economical because it is simple, highly efficient, regenerative, and scalable and does not produce intermediates that can increase the toxicity of the parent contaminants. Prompted by these reasons, in this research, an adsorbed medium composed of graphene oxide and an amine-oxazoline-based polymer (poly(2-(3-(amino)propyl))-2-oxazoline) was synthesized and employed in several adsorption experiments targeting nonsteroidal anti-inflammatory drugs such as ibuprofen (**1**), aspirin (**2**), ketoprofen (**3**), and benzoic acid (**4**). The specific interaction between acidic moieties of drugs and basic domains of the polymer has been investigated by targeting both acid compounds and pharmaceutical products free of carboxylic groups. Also, the influence of several parameters, including initial concentration, liquid-phase composition, pH, and reusability, has been investigated. Results show that the maximum adsorption capacity for ibuprofen (**1**), aspirin (**2**), ketoprofen (**3**), and benzoic acid (**4**) for experiments conducted in water, at the maximum initial concentration explored (90 mg L^{-1}) and at natural pH equilibrium (pH ∼ 4), are, respectively, 37.4, 27.5, 43.5, and 26.0 mg g^{-1}. These findings suggest that the prepared GO-pAmOx material has significant potential for adsorbing these drugs in water and good versatility for all investigated acid compounds and maintains high reusability. Notably, the reduction in adsorption capacity after ten adsorption cycles was only 1%.

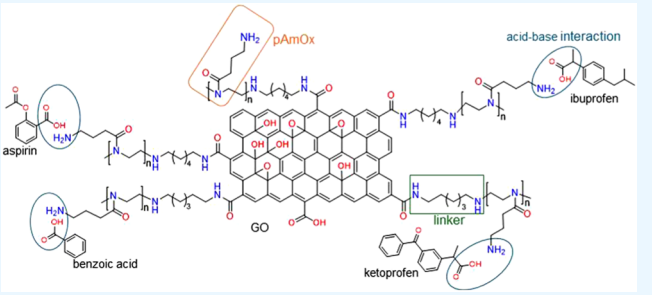

INTRODUCTION

Water is indispensable to both humans and wildlife, and the functioning of the world depends upon the availability of clean water.[1] Nowadays, global water demand continues to rise as a consequence of demographic growth, industrial needs, and evolving lifestyle.[2] An important source of anthropogenic pollution is represented by pharmaceuticals, hormones, consumer product chemicals, and other organic compounds (OWCs), employed in human activities and commonly detected in surface water, groundwater, and drinking water.[3−5] In particular, pharmaceuticals have caused great concern because, after their widespread consumption, traces of them or of their metabolites are excreted and reach the water resources either directly or after inefficient conventional wastewater treatment.[6] For the most part, several OWCs remain unregulated in drinking water, and existing toxicity data are insufficient to fully assess potential risks associated with chronic, low-dose exposure.[7] Such a dramatic scenario has motivated many governments and public health research institutions to focus their efforts on the monitoring of pharmaceutical residues and their effective removal from contaminated water sources. Starting from 2000, the EU Water Framework Directive (WFD, EC, 2000) and in 2008 the Priority Substances Directive (PSD, EC, 2008, 2013) also established a first list of priority pollutants that may pose a risk

Received: January 2, 2025
Revised: June 26, 2025
Accepted: July 1, 2025
Published: July 11, 2025

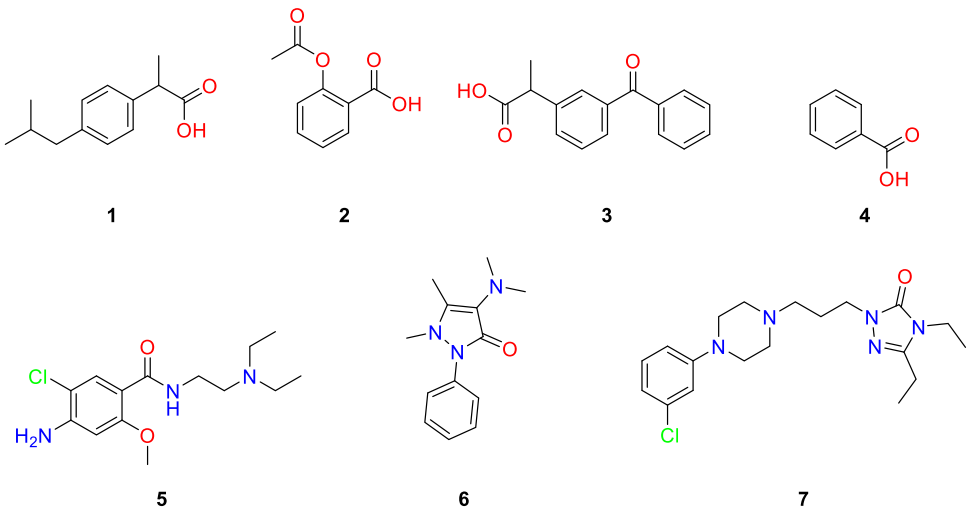

Figure 1. Pollutant pharmaceutical compounds commonly detected in wastewater: ibuprofen (**1**), aspirin (**2**), ketoprofen (**3**), benzoic acid (**4**), metoclopramide (**5**), pyramidone (**6**), and etoperidone (**7**).

to surface water and provide a legal basis for Member States to achieve Environmental Quality Standards (EQS) set for these substances.[8−10] Various methods have been explored for the removal of pharmaceuticals, with the aim of using low-cost technologies such as biodegradation, photocatalysis, ozonation, and Fenton process.[11] Nowadays the major removal mechanisms of these compounds in wastewater treatment plants (WWTPs) using biological approaches are conventional activated sludge treatment, membrane Bio-Reactor, attached growth, constructed wetland, algae photobioreactor, and stabilization ponds.[12] Most common systems aim to eliminate soluble organic pollutants, suspended solids, and flocculated matter, resulting in high-quality effluent suitable for environmental discharge. Nevertheless, current wastewater treatment systems are insufficiently effective or economical in removing persistent micropollutants. For instance, studies in southwestern India have reported the presence of common nonsteroidal anti-inflammatory drugs (NSAIDs), such as ibuprofen (**1**), aspirin (**2**), and ketoprofen (**3**), in three selected WWTPs effluent and river water (Gurupura River) at concentrations ranging from 5 to 22, 125 to 184, and 3 to 41 μg/L, respectively,[13] highlighting the limitations of conventional wastewater treatments.[8] Therefore, the development of novel, highly efficient, reusable, and biocompatible systems for OWC removal of organic pollutants by OWCs, even in traces, is not only crucial but also compulsory for human health and ecological well-being. Adsorption process has been found to be the most effective and economical due to its simplicity, scalability, and potential of regeneration without generating byproducts that can increase the toxicity of the parent contaminants.[14] The ideal and suitable adsorbent should possess a large surface area, high capacity and ability to adsorb, appropriate pore size and volume, comfortable accessibility, efficiency, cost effectiveness, robust mechanical stability, biocompatibility, and ready regenerability.[15] Encouraged by previous successful efforts from our laboratories in this field, we devised the possibility of synthesizing a biopolymeric-based adsorbent material for the removal of selected organic pollutants. In this challenge, poly(2-oxazoline)s, known for their biocompatibility,[16−18] synthetic versatility, and stealth behavior,[19−21] have been selected as the polymeric backbone. In fact, polyoxazoline-based material has been employed to catch heavy metal ions[22] and also organic pollutants.[23,24] As a supporting material for polymer, graphene oxide (GO) becomes a suitable substrate due to its mechanical strength and low chemical degradability.[25] Additionally, GO has oxygen functional groups such as carboxyl, carbonyl, epoxy, and hydroxyl that can lead to surface modification turning to be reactant specific for various organic entities.[26,27] Knowing that, we devoted several efforts to designing and synthesizing a polymeric-based adsorbent capable of interacting with NSAIDs and covalently linking it onto GO. This study investigates the adsorption of a series of pharmaceutical compounds onto a polyoxazoline-based polymer, properly functionalized with an amine moiety, hypothesizing possible interactions with the carboxyl groups of small acidic drugs, such as ibuprofen (**1**), aspirin (**2**), and ketoprofen (**3**). We considered also, as a pollutant, benzoic acid (**4**) as a further representative pollutant due to its well-known carcinogenic and toxic properties at certain concentrations and its widespread use, primarily in food, cosmetic, and pharmaceutical-related products.[28] To test and validate our hypothesis, we also included in our investigations nonacidic compounds, i.e., metoclopramide (**5**), pyramidone (**6**), and etoperidone (**7**), expecting for them a very low adsorption. The structures of all compounds employed in the initial adsorption experiments are listed in Figure 1.

RESULTS AND DISCUSSION

Preparation of the Adsorbent Material. In this research, a novel composite material was synthesized by covalently linking poly(2-(3-(Boc-amino)propyl)-2-oxazoline) (Boc-protected pAmOx, DP = 25), the preparation of which has been reported in a previous research from us to graphene oxide (GO), obtained from the modified Hummers method[29] (Scheme 1).

The synthetic pathway involves the cationic ring-opening polymerization of the BocOx monomer (**9**), followed after 48 h by chain-end-capping with 1,6-hexanediamine (**11**). The resulting amine-terminated polymer was allowed to react with GO in the presence of *N,N′*-dicyclohexylcarbodiimide (DCC) as coupling agent to afford the desired composite material in a quite good overall yield (for details, see the Experimental Section). After Boc deprotection, realized by overnight stirring

https://doi.org/10.1021/acsomega.5c00043
ACS Omega 2025, 10, 30087−30099

Scheme 1. GO-pAmOx Synthetic Pathway

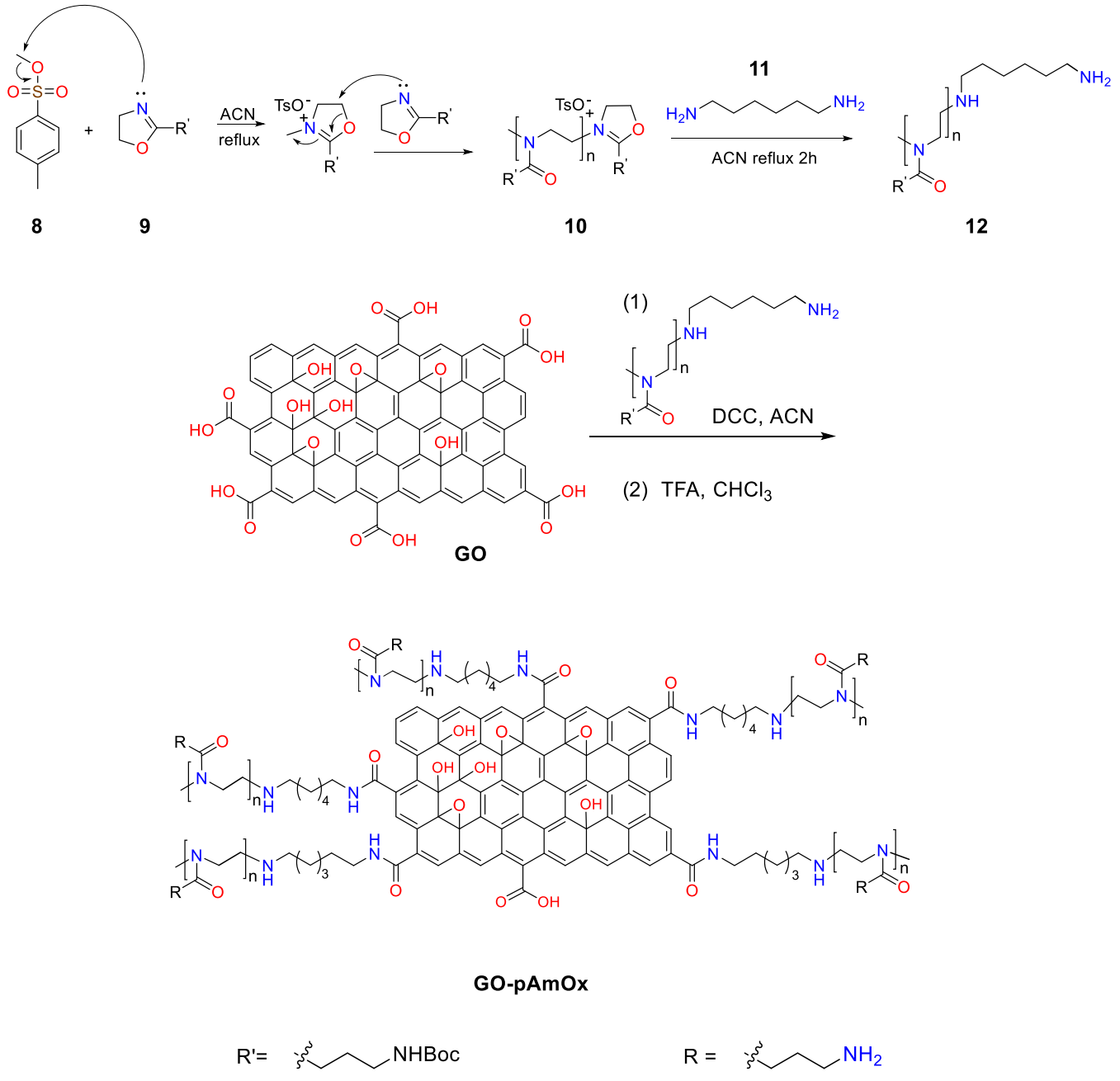

of the material, dispersed in chloroform, in the presence of trifluoroacetic acid, the obtained GO-pAmOx was washed with tetrahydrofuran (THF) until no more polymer was found in the supernatant, recovering GO-pAmOx as precipitate after centrifugation. After the preparation and purification, GO-pAmOx was thoroughly characterized and evaluated for its adsorption, targeting common organic pollutants. To rigorously assess its performance, pollutant concentrations even significantly higher than those typically found in wastewater were employed.

The GO-pAmOx's structure, thermal properties, morphology, and composition were investigated through thermogravimetric analysis (TGA), infrared spectroscopy FTIR (ATR), atomic force microscopy (AFM), and transmission electron Microscopy (TEM) associated with electron energy loss spectroscopy (EELS).

Characterization of the Adsorbent. *ATR-FTIR Analysis.* Since the primary objective of our study was to assess the successful linkage of the polymer onto the GO substrate, we identified Fourier transform infrared (FTIR) spectroscopy as a more robust and widely endorsed technique. This method provides direct insights into the chemical bonds and functional groups present, thereby offering comprehensive data on the structural conjunction achieved. In our research, ATR-FTIR absorption spectra of GO, pAmOx, and GO-pAmOx are compared in Figure 2. The free pAmOx polymer and GO-pAmOx show similar characteristics in the absorption profile, indicating that the GO infrared absorption has been modified by the polymer linkage, with respect to the starting material. Indeed, the final spectrum of the GO-pAmOx composite exhibits characteristics indicative of a superposition of the individual component spectra. Specifically, the following

https://doi.org/10.1021/acsomega.5c00043
ACS Omega 2025, 10, 30087−30099

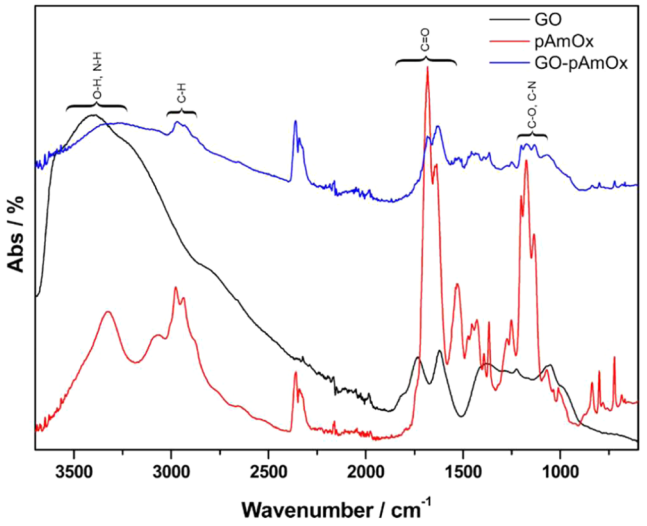

Figure 2. ATR-FTIR spectra for GO, pAmOx, and GO-pAmOx with main diagnostic regions labeled.

features are discernible: (i) the broad band in the 3450−3250 cm^{-1} region is primarily attributed to O−H stretching vibrations, characteristic of GO, coupled with N−H stretching vibrations arising from the polymer's contribution; (ii) the C−H sp^3 stretching vibrations from the polymer are evident at 2978 and 2938 cm^{-1}, (iii) the carbonyl absorption at 1679 cm^{-1} is diagnostic of the amide bond formation, exhibiting a clear shift compared with the C═O stretching vibration at 1733 cm^{-1} observed in the spectrum of pristine GO; (iv) in the region between 1560 and 1355 cm^{-1}, C−H bending vibrations from the polymer side chains, along with other skeletal vibrations, are observed, features largely absent in the spectrum of original GO; (v) the C−N and C−O stretching vibrations at 1220, 1170, and 1136 cm^{-1} are present in the spectrum of the poly(2-oxazoline) homopolymer (plotted as reference) but absent in the GO spectrum.

Thermogravimetric Analysis. To investigate composite material thermal properties, thermogravimetric analysis (TGA) is usually performed to observe if any change from the thermal behavior of the starting material could be observed, revealing that the desired modification occurred. Figure 3a depicts the relationship between weight loss and temperature for GO, pAmOx, and GO-pAmOx with their derivatives (DTG) in Figure 3b−d. The TGA curve of prepared graphene oxide (GO) exhibits (i) a 6% weight loss up to 100 °C associated with the thermal desorption of water molecules, physically adsorbed onto the hydrophilic GO surface; (ii) a sharp weight loss (80%) between 100 and 200 °C because of the decomposition of oxygen-containing functional groups to CO, CO_2, and H_2O;[30] and (iii) a 6% weight loss up to 800 °C, associated with the removal of more thermally stable oxygen functionalities and thermal decom-

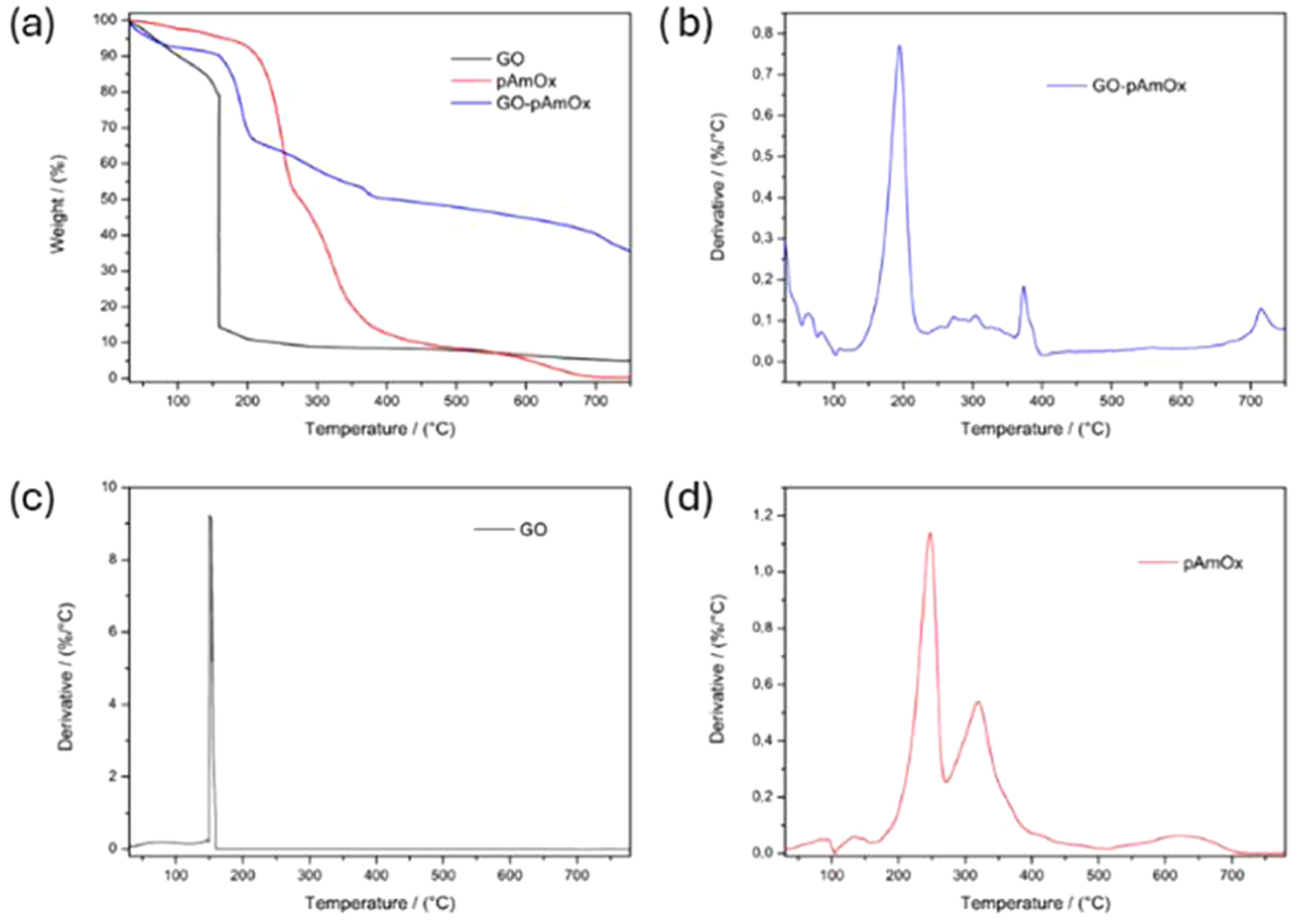

Figure 3. (a) TGA analyses for GO, pAmOx, and GO-pAmOx, the first derivative of weight loss for GO-pAmOx (b), GO (c), and pAmOx (d).

https://doi.org/10.1021/acsomega.5c00043
ACS Omega 2025, 10, 30087−30099

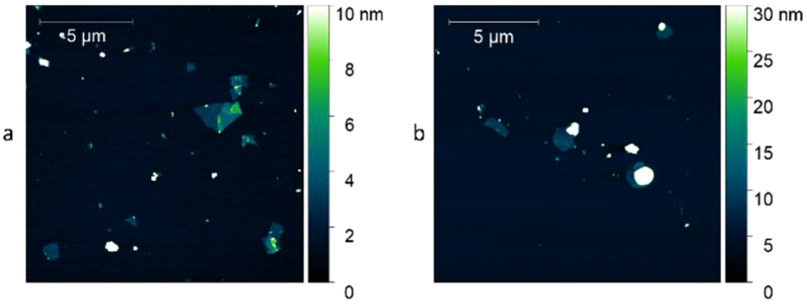

Figure 4. 15 × 15 μm^2 AFM images of GO (a) and GO-pAmOx (b) where the height of the sample is given by the color scale on the right.

position of GO. The observed curve (for solely GO) is similar to that reported in the publications by Ohno et al.[31] and Wang et al.[32] in which composite materials, based on GO and organic polymers, have been investigated also through this analytical technique. Quite the opposite, the simple polymer (pAmOx) exhibits a strong weight loss (90%) up to 500 °C and a smaller one between 500 and 800 °C, with no remaining ashes. The shape of the thermal decomposition curve for the GO functionalized with the polymer (GO-pAmOx) shows substantial variations, respectively, to GO and pAmOx. Indeed, the sample exhibited a four-stage weight loss profile: ca. 7% below 100 °C, ca. 20% between 100 and 200 °C, and ca. 20% between 200 and 500 °C, resulting in a high ashes residuum up to 800 °C. The reported outcome clearly indicates the successful covalent functionalization of GO, although a precise quantification of the pAmOx loading remains challenging.

Atomic Force Microscopy (AFM) Analysis. The AFM investigation of GO and GO-pAmOx involved acquiring large-field scans ranging from 10 × 10 to 50 × 50 μm^2 to ensure a representative sampling of the materials. Both GO and GO-pAmOx appear as randomly distributed flakes, with GO-pAmOx showing a more dispersed distribution compared with GO. The height of both samples varies from approximately 5 to 50 nm, proving that the sonication process exfoliated the flakes at different sizes and heights. In terms of morphology, GO flakes are characterized by ridges with an average roughness of about 10 nm and exhibit sharp edges. In contrast, GO-pAmOx flakes are flatter, with a roughness of approximately 3 nm, and display more rounded features, as shown in Figure 4. The different morphology and roughness could be attributed to the presence or absence of pAmOx on the samples. Indeed, GO layers typically break as they exfoliate, leading to an increased roughness. On the contrary, GO-pAmOx single layers appear to entirely exfoliate during the sonication, resulting in a smooth surface.

Transmission Electron Microscopy (TEM) and Electron Energy Loss Spectroscopy (EELS). To elucidate the morphology and determine the elemental composition of GO and GO-pAmOx composite, we conducted an extensive examination using TEM with subangstrom resolution, complemented by EELS analyses. Indeed, the presence of both organic groups on the surface and the polymer grafted onto the graphene oxide (GO) gives this material a mixture of sp^2 and sp^3 carbon, in contrast to the well-ordered structures of pure GO, graphene, and graphite. The resulting amorphous structure underscores the preference for TEM and EELS, given their superior capabilities in analyzing noncrystalline materials over other techniques more suitable for crystalline structures. Concerning morphological analyses, GO and GO-pAmOx do not show noticeable differences, as shown by Figure 5a,b. It is crucial to note that all analyses are performed under vacuum conditions, without the presence of any solvents that could alter the GO sheets in terms of morphology. The GO and GO-pAmOx chemical compositions were also investigated by EELS technique. Figure 5c,d presents the EELS spectra acquired for GO and GO-pAmOx, respectively. In the first case, only two peaks are detected at 281 and 528 eV due to the presence of carbon and oxygen of the GO sheets. The inset of Figure 5c shows a magnified region between 300 and 700 eV where it is clearly evident the absence of any signals related to nitrogen around 400 eV. In the GO-pAmOx EELS spectra (Figure 5d), the presence of nitrogen is attested by the appearance of a third peak at 396 eV due to the presence of the nitrogen atoms of the pAmOx polymer. In the magnified region, shown in the inset of Figure 5d, it is possible to clearly see the signals related to the presence of the nitrogen atoms that are almost comparable in intensity to the oxygen one.

Moreover, in Figure 5e,f, a TEM image and its related nitrogen signal intensity map, acquired by EELS analyses, are shown. As can be seen, the nitrogen signal is uniform all over the GO sheets, testifying that the polymer is grafted uniformly on all of the GO sheets and attesting to the strong interaction between the polymer anchoring group and the GO surface moieties.

Batch Adsorption Experiments. To investigate the adsorption performances of GO-pAmOx, batch adsorption experiments were initially conducted in water:methanol (70:30) solution. Briefly, 10 mg of adsorbent materials (either GO or GO-pAmOx) was added to 5 mL of each drug solution (concentrations ranged from 25 to 250 mg L^{-1}) and after 12 h the residual concentrations of pharmaceutical products were evaluated with HPLC analyses (for details, see the Experimental Section). Experiments were conducted in triplicate for each pharmaceutical compound, using GO, GO-pAmOx, and control samples (no adsorbent added) to directly compare the adsorption properties and efficiencies. Adsorption capacity [q_e (mg g^{-1})] was determined using eq 1, which relates the amount of adsorbed pollutant to the amount of the employed adsorbent. Specifically

$$q_e = \frac{(C_0 - C_e)V}{W} \quad (1)$$

where C_e (mg L^{-1}) is the experimental liquid-phase concentration of pharmaceutical at equilibrium, C_0 (mg L^{-1}) is the average concentration of pharmaceutical in the corresponding control, V is the volume of the solution (L), and W is the amount (g) of the adsorbent used. In Figure 6 we report the adsorption coefficient q_e as a function of the initial concentration, along with a table listing the log P values of the pharmaceutical compounds to aid in the analysis of the

https://doi.org/10.1021/acsomega.5c00043
ACS Omega 2025, 10, 30087−30099

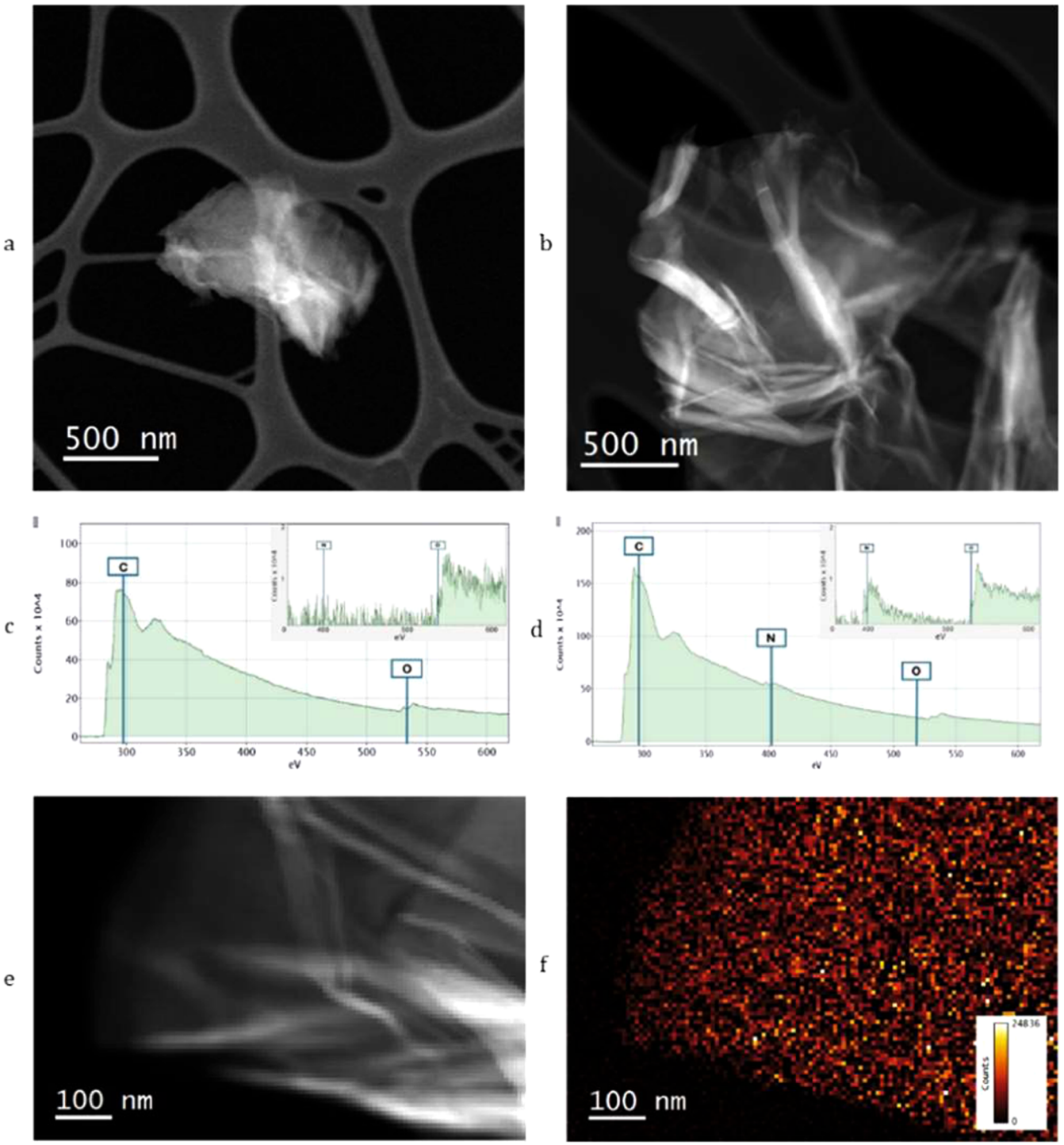

Figure 5. TEM images of GO (a) and GO-pAmOx (b). EELS spectra of GO (c) and GO-pAmOx (d) with the magnified region between 300 and 600 eV (insets). TEM images related to the EELS analyzed area of GO-pAmOx (e) and EELS nitrogen distribution map (f).

correlations. Our data show a compelling contrast in the adsorption of ibuprofen (**1**), aspirin (**2**), ketoprofen (**3**), and benzoic acid (**4**) significantly favored by GO-pAmOx over GO, with respect to the opposite behavior observed for metoclopramide (**5**), pyramidone (**6**), and etoperidone (**7**). An examination of Figure 1 reveals that the presence of aromatic rings strongly promotes the interaction with GO layers via $\pi-\pi$ stacking, which facilitates the removal of all of the tested pharmaceuticals (**1**–**7**).

Notably, the distinct differences in adsorption capacities between the GO-pAmOx composite and pure GO should be primarily attributed to the interplay between carboxylic moieties, a common feature in compounds **1**–**4**, and amine functionalities, which are ubiquitous in compounds **5**–**7**. Specifically, at the maximum initial concentration explored (250 mg L^{-1}), GO-pAmOx yields impressive q_e values of 28.0, 49.8, 65.0, and 17.0 mg g^{-1}, respectively, for ibuprofen (**1**), aspirin (**2**), ketoprofen (**3**), and benzoic acid (**4**). In contrast, the corresponding q_e values for these compounds when using

https://doi.org/10.1021/acsomega.5c00043
ACS Omega 2025, 10, 30087−30099

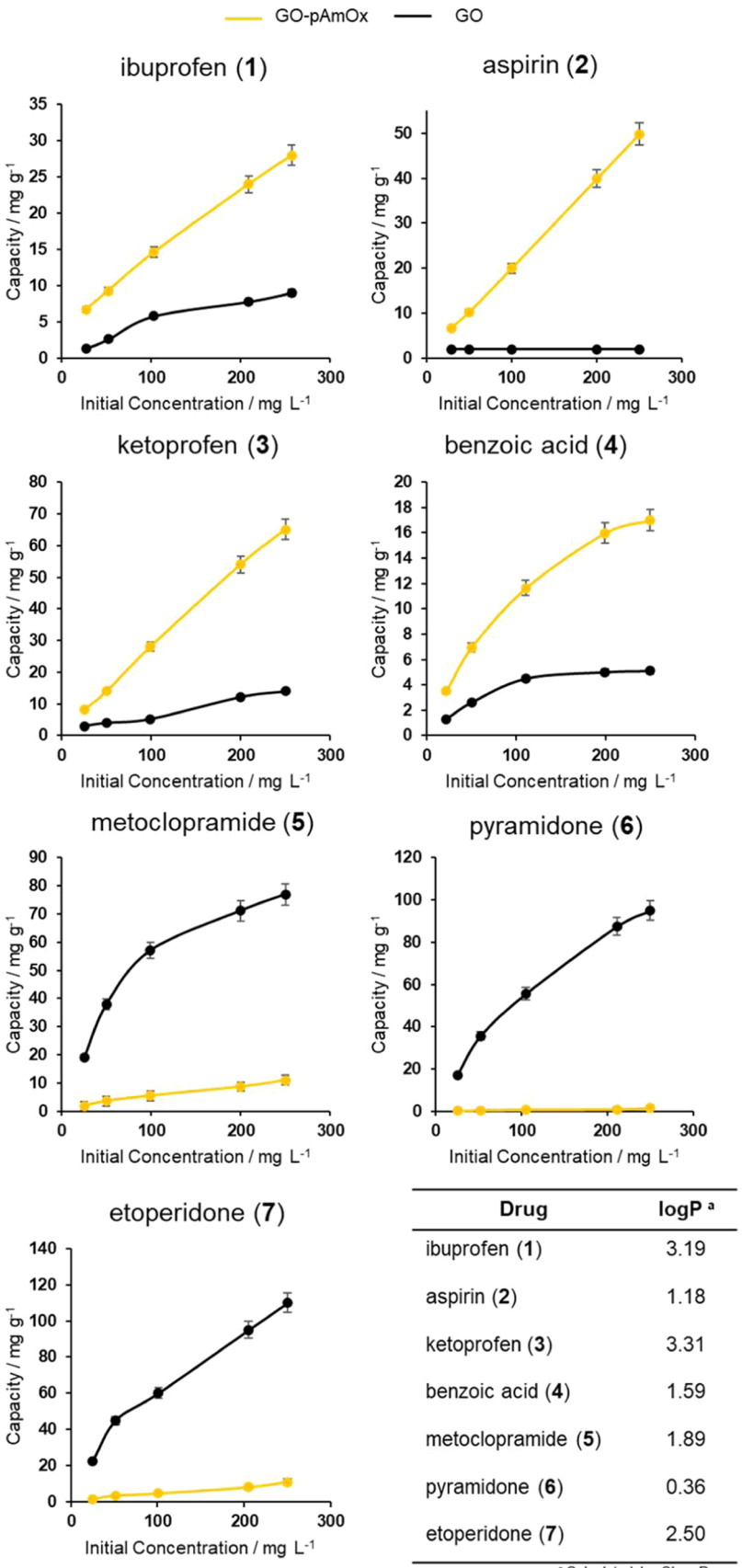

Drug	logP [a]
ibuprofen (**1**)	3.19
aspirin (**2**)	1.18
ketoprofen (**3**)	3.31
benzoic acid (**4**)	1.59
metoclopramide (**5**)	1.89
pyramidone (**6**)	0.36
etoperidone (**7**)	2.50

[a] Calculated by ChemDraw

Figure 6. q_e vs initial concentration for each drug in adsorption experiments conducted in hydroalcoholic medium and log *P* values table.

pure GO are substantially lower, measuring 9.0, 2.0, 14.0, and 5.1 mg g^{-1}. This disparity underscores the importance of acid−base interactions between the amino groups of pAmOx and the acidic groups of compounds **1**−**4**, which substantially enhance

https://doi.org/10.1021/acsomega.5c00043
ACS Omega 2025, 10, 30087−30099

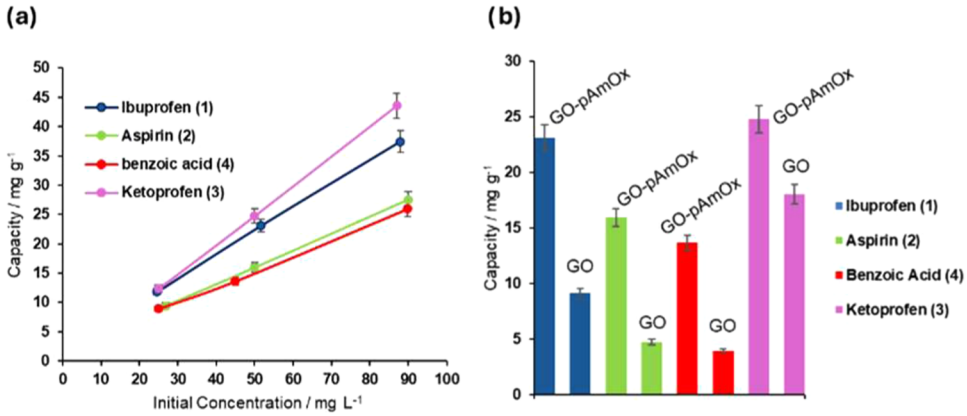

Figure 7. (a) q_e vs initial concentration for each drug in adsorption experiments conducted in water. (b) q_e comparison between GO-pAmOX and GO for each drug in water adsorption experiments at 50 mg L^{-1} as the initial concentration.

the adsorption affinity of the GO-pAmOx composite, thereby strengthening the overall adsorption process. Meanwhile, the repulsion due to the carboxylic functions that decorate the pure GO surface negates any alternative positive interactions that could occur between compounds **1**−**4** and GO. In the case of metoclopramide (**5**), pyramidone (**6**), and etoperidone (**7**), the absence of carboxylic moieties strongly diminished their affinity for the composite GO-pAmOx resulting in notably lower q_e values of 11.0, 1.4, and 11.0 mg g^{-1}. However, when tested with pure GO, the presence of various amine functionalities strongly fosters additional acid−base interactions, which, coupled with possible halogen bonding with the sp^2 carbon atoms of GO, yields striking q_e values of 77.0, 95.0, and 110.0 mg g^{-1}. In addition to the acid−base interactions, the higher hydrophobicities of ibuprofen (**1**) and ketoprofen (**3**) must be considered. These compounds possess significantly higher log P values (3.19 and 3.31, respectively) compared with aspirin (**2**) and benzoic acid (**4**) (1.18 and 1.59, respectively), rendering them more compatible with the less hydrophilic GO-pAmOx surface in the aqueous environment, and resulting in elevated q_e values. By leveraging these synergistic interactions, our findings not only reinforce the usefulness of GO as an adsorbent but also highlight the enhanced selective removal capabilities of the GO-pAmOx composite for organic pollutants in aqueous environments. This underscores its remarkable potential for advanced applications in water remediation. Given our aim to develop a material for water remediation, the adsorption performance of GO-pAmOx was investigated in aqueous solutions limiting our experiments to compounds **1**−**4** (Figure 1), selected based on their preferential adsorption onto GO-pAmOx in hydroalcoholic media. Figure 7a depicts the adsorption capacity (q_e) as a function of the initial concentration, ranged from 25 to 90 mg L^{-1} for each drug. The concentrations explored fall in the linear range of the adsorption trend as evident from the high R^2 values (>0.99) obtained from the linear fitting of the data for all compounds. At the maximum initial concentration tested (90 mg L^{-1}), the adsorption coefficient values were 37.4, 27.5, 43.5, and 26.0 mg g^{-1} for ibuprofen (**1**), aspirin (**2**), ketoprofen (**3**), and benzoic acid (**4**), respectively. For comparison, equivalent experiments were conducted with GO alone at 50 mg L^{-1}, and the results are illustrated in Figure 7b.

Aqueous adsorption experiments (50 mg L^{-1} initial concentration) confirm the superior adsorption capacity of GO-pAmOx compared with that of GO for compounds **1**−**4** (Figure 7 and Table 1). Specifically, the q_e values for GO-pAmOx were 23.1, 15.9, 24.8, and 13.6 mg g^{-1} for ibuprofen (**1**), aspirin (**2**), ketoprofen (**3**), and benzoic acid (**4**), respectively, significantly greater than the values obtained with GO (9.1, 4.7, 18.0, and 3.9 mg g^{-1}). Analogously to what was observed in the hydroalcoholic medium, this enhanced adsorption could be attributed to the synergistic effect of $\pi-\pi$ stacking (between the aromatic rings and GO) and acid−base interactions (between the carboxylic acid groups and the amine moieties of pAmOx). Therefore, while the $\pi-\pi$ stacking interaction alone contributed to some degree to the adsorption with GO, the derivatization with pAmOx dramatically improves the adsorption by providing a second strong interaction pathway. Importantly, the q_e values measured in pure water (at the same initial concentration) were higher than those obtained in water:methanol (70:30) (Table 1). Such behavior is consistent with the decreased aqueous solubility of these pharmaceutical compounds in water, thus rendering them more susceptible to adsorption (which is also true for the case of GO alone as the adsorbent).

Table 1. Adsorption Coefficient (q_e) in mg g^{-1} in Different Solvents at 50 mg L^{-1} as the Initial Concentration

	H_2O/CH_3OH (70:30)		H_2O	
drug	GO-pAmOx	GO	GO-pAmOx	GO
ibuprofen (**1**)	9.3	2.6	23.1	9.1
aspirin (**2**)	10.2	2.0	15.9	4.7
ketoprofen (**3**)	14.0	4.0	24.8	18.0
benzoic acid (**4**)	7.0	2.6	13.6	3.9

Along the same lines, it is interesting to note that the adsorption of ibuprofen (**1**) is enhanced in water. In fact, it is more easily adsorbed than aspirin (**2**), whereas in the hydroalcoholic environment, the trend is reversed. This is probably due to its high hydrophobicity, compared with aspirin (**2**) (see the log P table in Figure 6). Such evidence suggests that while experiments in hydroalcoholic mixtures allow one to explore higher concentrations of drugs due to the increased solubility, experiments in water are also necessary to understand adsorption processes in a more realistic matrix. To further validate the observed selectivity, we conducted additional adsorption experiments with a mixture of the selected acidic drugs **1**−**4** in an aqueous solution (see SI,

https://doi.org/10.1021/acsomega.5c00043
ACS Omega 2025, 10, 30087−30099

Figure S5). These experiments confirmed the previously observed trend, with ketoprofen (3) and ibuprofen (1) exhibiting the highest adsorption, while aspirin (2) and benzoic acid (4) demonstrated comparatively lower removal rates. Although the individual adsorption coefficients remained consistent with those obtained in single-component experiments, the overall q_e values were modestly reduced, likely due to the establishment of a more complex and heterogeneous adsorption/desorption equilibrium within the multicomponent system, where competition for available binding sites is anticipated.

Adsorption Isotherms. To study how ibuprofen (1), aspirin (2), ketoprofen (3), and benzoic acid (4) distribute between the liquid and the adsorbent phases, the data of equilibrium adsorption capacity for GO-pAmOx were analyzed according to Langmuir and Freundlich models of adsorption isotherms. The type 2 Langmuir isotherm model can be expressed in a linearized form as follows (eq 2)

$$\frac{1}{q_e} = \frac{1}{K_L q_{max}} \frac{1}{C_e} + \frac{1}{q_{max}} \quad (2)$$

where K_L is the Langmuir constant, which provides a measure of the binding affinity and q_{max} is the maximum adsorption capacity.[33]

The Freundlich isotherm model can be expressed as follows (eq 3)

$$\ln q_e = \ln K_F + \frac{1}{n} \ln C_e \quad (3)$$

where K_F is the Freundlich constant that, similarly to K_L, provides a measure of the binding affinity, and n is a parameter that quantifies the heterogeneity of adsorption.[34] The Langmuir model assumes monolayer adsorption (i.e., layers of only one adsorbed molecule for each site), where all of the adsorption sites are equivalent and have the same affinity for the adsorbed molecule, i.e., adsorption is homogeneous. Instead, the Freundlich model can be applied to multilayer adsorption, and heterogeneity is considered (heterogeneous surface and/or adsorption sites and/or affinity for the ligand). According to eqs 2 and 3, the parameters of the two models can be obtained from the linear regression of $1/q_e$ vs $1/C_e$ and $\ln q_e$ vs $\ln C_e$, as reported in Table 2. In the same table, also the value of R^2 is reported as a measure of the goodness of each linear fit. Analysis of the adsorption isotherms (Table 2) using both Langmuir and Freundlich models yielded excellent fits ($R^2 > 0.9$) for all four compounds. In detail, the Freundlich model provided a superior fit, i.e., the best correlation coefficients with respect to the Langmuir one, for both ibuprofen (1) and aspirin (2), while both models performed similarly for ketoprofen (3), differently for benzoic acid (4) the Langmuir model showed a marginally better fit. The Langmuir q_{max} values (mg g^{-1}) correspond to 27, 78, 27, and 68, respectively, for ibuprofen (1), aspirin (2), benzoic acid (4), and ketoprofen (3). These values are consistent with the experimental adsorption capacities calculated at the highest concentration explored. Freundlich n values between 1 and 10 suggest remarkably favorable adsorption for each compound.[35] Similarly, the K_F and K_L values confirm that GO-pAmOx has the strongest affinity for ketoprofen (3). However, the very high R^2 values obtained for both fitting procedures preclude a definitive determination of both the precise adsorption mechanism (monolayer versus multilayer) and the assessment of the heterogeneity or homogeneity of the adsorption sites.

Table 2. GO-pAmOx Langmuir and Freundlich Parameters for Hydroalcoholic Medium Experiments

Langmuir Isotherm Model			
drug	q_{max} (mg g^{-1})	K_L (L mg^{-1})	R^2
ibuprofen (1)	27 ± 7	0.023 ± 0.009	0.921
aspirin (2)	78 ± 30	0.006 ± 0.002	0.965
ketoprofen (3)	68 ± 16	0.033 ± 0.007	0.989
benzoic acid (4)	27 ± 2	0.009 ± 0.001	1.000
Freundlich Isotherm Model			
drug	n	K_F (L mg^{-1})	R^2
ibuprofen (1)	1.7 ± 0.2	1.4 ± 0.3	0.975
aspirin (2)	1.3 ± 0.2	0.6 ± 0.1	0.988
ketoprofen (3)	1.7 ± 0.1	3.8 ± 0.5	0.988
benzoic acid (4)	1.6 ± 0.2	0.7 ± 0.2	0.971

Evaluation of the pH Effect on the Adsorption Process. Given the presence of carboxylic acid groups in the target pharmaceuticals and basic amine groups in the pAmOx component of the composite, the influence of pH on adsorption in water was investigated at 90 mg L^{-1} (the maximum concentration used in the aqueous adsorption experiment at the natural pH equilibrium; Figure 8).

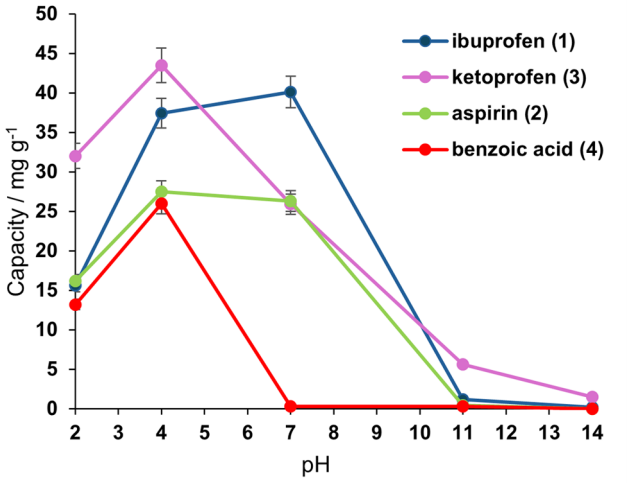

Figure 8. q_e vs pH in water experiments at 90 mg L^{-1} as the initial concentration.

The pH of the prepared solutions was adjusted to the desired value by the addition of 0.1 M NaOH or HCl. Maximum adsorption (q_e) is achieved at natural pH equilibrium (approximately pH 4) for ketoprofen (3) and benzoic acid (4). Concerning ibuprofen (1) and aspirin (2), the maximum adsorption was achieved not only at pH ∼ 4 but also remains high even at pH 7. A marked reduction in q_e is observed as the pH decreases below pH 4 ascribable to the protonation of the amine groups within the GO-pAmOx composite, thereby suppressing the acid−base interactions with the carboxylic acid groups of the pharmaceuticals. The significant reduction in q_e at pH values exceeding 7 is likely due to the deprotonation of pharmaceutical compounds' acidic groups, making them unable to interact with the polymer's active amine moieties.

https://doi.org/10.1021/acsomega.5c00043
ACS Omega 2025, 10, 30087−30099

Reusability. The reusability of adsorbents is a key characteristic to consider and evaluate, but it is often overlooked during the development of new materials. To be reused, the adsorbent should successfully release the contaminant by a desorption or regeneration step without compromising the chemical and physical stability of the matrix.[36] To assess the reusability of the prepared GO-pAmOx as an adsorbent, ten consecutive adsorption−desorption cycles were performed employing polluted solutions of compounds **1**−**4** in water adsorption experiments at 90 mg L^{-1} as an initial concentration. Following each adsorption step, GO-pAmOx (10 mg) was washed successively with tap water (3 × 10 mL), distilled water (3 × 20 mL), and finally with methanol (10 mL), recovering the adsorbent material, after each washing step, through centrifugation (5000 rpm, 10 min) and vacuum drying. After the regeneration step, the adsorbent material was loaded again with 5 mL of the drug's water solution. The adsorption capacity (q_e) was recalculated following each regeneration cycle. Figure 9 demonstrates that a negligible

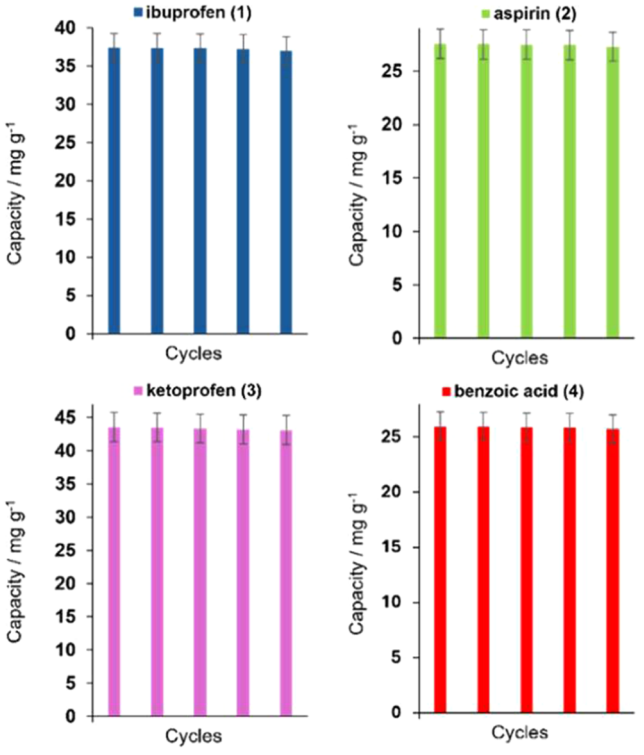

Figure 9. q_e calculated for the loading cycles (each bar represents two adsorption cycles) employing the highest initial concentration.

reduction in q_e of less than 1% was observed after ten cycles, highlighting the exceptional reusability and stability of the composite material. The structural integrity of the regenerated GO-pAmOx was further validated by post-regeneration TGA and ATR (FTIR) analyses (results are presented in SI).

EXPERIMENTAL SECTION

Materials, Chemicals, and Instrumentation. The Supporting Information provides full details of materials, chemicals, and instrumentation used.

Synthesis of *tert*-Butyl (3-(4,5-Dihydrooxazol-2-yl)-propyl)carbamate BocOx 9. The synthesis of BocOx (**9**) is reported in the Supporting Information and the characterization is consistent with the literature.[22,37]

Preparation of Poly(2-(3-(Boc-amino)propyl))-2-Oxazoline (12). A two-neck round-bottom flask equipped with an efficient reflux condenser and a magnetic stir bar was charged with BocOx (**9**) (20 mmol) and anhydrous ACN (12 mL). The system was kept under an argon atmosphere, 600 μL of a solution 1:10 methyl tosylate (**8**):ACN was added to start the polymerization, and the reaction mixture was stirred for 48 h at 90 °C. After, the reaction was quenched by the addition of 10 equiv of initiator of 1,6-hexanediamine (**11**) solution in anhydrous ACN (4 mL), and the resulting mixture was stirred at the same temperature for 2 h. Finally, the solvent was reduced under vacuum and the residue was added to a solution of petroleum ether:diethyl ether (1:1). The polymer was recovered as a white precipitate, the supernatant was removed, and the product was washed twice with the petroleum ether:diethyl ether solution and dried in vacuo. Finally, the polymer was dialyzed (cut off 3.5 kDa) against methanol for 5 days changing the solvent 10 times. Yield is 85%.

GPC (*N*,*N* dimethylformamide (DMF) with LiBr (0.05 M)): 5.8 kDa, $Đ$ = 1.1.

Preparation of Graphene Oxide (Modified Hummers Method). Graphene oxide (GO) was prepared with the modified Hummers method. Specifically, graphite (5 g) and 3.8 g of $NaNO_3$ are introduced into a 2 L flask equipped with a magnetic stir bar. Then, H_2SO_4 (375 mL) was added at 0 °C (ice bath), and the solution was stirred until it was homogeneous (1 h). $KMnO_4$ (25 g) was slowly added over 1 h, keeping the temperature below 10 °C. After 2 h, the solution was allowed to warm to room temperature and was stirred. After 5 days (color change from dark green to brown) 700 mL of H_2SO_4 (5%) was added dropwise, keeping the temperature below 40 °C and the mixture was stirred for 2 h. Then 20 mL of H_2O_2 (30%) was added dropwise. After 2 h, the solution was diluted to 2 L with 5% H_2SO_4 and after 1 day of sedimentation, 1 L of the supernatant was removed and replaced with water (1 L), and 10 mL of H_2O_2 (30%) was added. After 18 h of sedimentation, the supernatant was removed, and the solid was washed with 5% H_2SO_4 and 0.3% H_2O_2 solution (12 times), then with HCl 4% (3 times), and finally with deionized water (10 times). The solid was filtered and washed with deionized water, suspended in acetone, and recovered after centrifugation. The product was dried in vacuo before use.

Preparation of the Adsorbent Material (GO-pAmOx). A two-neck round-bottom flask equipped with an efficient reflux condenser and a magnetic stir bar was charged with Boc-protected pAmOx (**12**) (1.4 g), 400 mg of DCC, 450 mg of GO, and anhydrous ACN (30 mL). The system was sonicated for 1 h, then placed in an oil bath at 90 °C, and stirred overnight. After, the solvent was removed with a rotatory evaporator, and the precipitate was washed three times with tetrahydrofuran (THF) and recovered after centrifugation. GO-pAmOx was deprotected by stirring the substrate, dispersed in anhydrous $CHCl_3$, overnight after the addition of 400 μL of TFA. The solvent was removed under vacuum and the final product was washed three times again with THF to remove undesired byproducts and the unattached polymer. Finally, GO-pAmOx was recovered after centrifugation (yield: 910 mg, with an approximate weight increase of 100% with respect to the pristine GO).

https://doi.org/10.1021/acsomega.5c00043
ACS Omega 2025, 10, 30087−30099

Preparation of Pharmaceutical Stock Solutions. The proper amount of pharmaceutical compound was weighed and transferred in a conical flask equipped with a magnetic stir bar, then the solvent (hydroalcoholic mixture or water) was added, and the system was hardly stirred under heating at 35 °C in an oil bath. After complete dissolution of the drugs, the solution was cooled to 25 °C and employed in adsorption experiments.

Adsorption Experiments. Adsorption experiments were done in triplicate under batch operation conditions targeting pharmaceutical compounds. First, an amount of 10 mg of GO-pAmOx (or GO) was added to 6 mL reaction tubes. Then, 5 mL of standard solutions with concentrations ranging from 25 to 250 mg L^{-1} were loaded into the cartridge. To allow homogeneous adsorption on the polymer surface, the tubes were incubated in a thermostatic shaker (50 rpm for 12 h). Triplicate controls, which consisted of solutions of the corresponding pharmaceutical in the absence of any adsorbent and in the same conditions, were run in parallel. Finally, the supernatants were filtered using PTFE filters, transferred into glass vials, and analyzed by HPLC-DAD.

CONCLUSIONS

In summary, we have presented the successful achievement and thorough characterization of a novel composite material composed of graphene oxide (GO) and poly(2-(3-(amino)-propyl))-2-oxazoline (pAmOx). Comprehensive characterization, utilizing TGA, ATR-FTIR, AFM, and TEM-EELS, validated the successful covalent functionalization of graphene oxide (GO) with the amine-functionalized polyoxazoline (pAmOx) and evaluated thermal, physicochemical, and morphological properties of the synthesized adsorbent. Subsequently, the obtained composite material was employed in several pharmaceutical product adsorption experiments, targeting the most common pollutants normally detected in wastewater. GO-pAmOx demonstrated significantly enhanced adsorption capabilities for selected acidic pharmaceuticals [ibuprofen (**1**), aspirin (**2**), ketoprofen (**3**), and benzoic acid (**4**)] compared with both pure GO and previously reported adsorbents. This enhancement arises from a synergistic interplay between $\pi-\pi$ stacking interactions with the aromatic rings of the pharmaceuticals and acid−base interactions with the pAmOx amine moieties. Importantly, this cooperative effect yields a marked selectivity for acidic compounds, showcasing the potential for targeted pollutant removal. Furthermore, GO-pAmOx exhibited exceptional reusability, maintaining high adsorption efficiency over multiple cycles (only a 1% decrease in q_e was observed after ten reuse cycles). Evaluation in aqueous media, under environmentally relevant conditions, confirmed the promising practical applicability of the newly synthesized adsorbent for water purification. The adsorption behavior was systematically investigated, elucidating the influence of initial concentration and pH. The results obtained surpass those observed with previously reported materials. Indeed, the obtained q_e values for both ketoprofen (**3**) and ibuprofen (**1**) result to be higher than the reported ones for molecular imprinted polymer[38] and for mesoporous silica SBA-15.[39] In conclusion, the presented study highlights GO-pAmOx as a highly effective and sustainable solution for advanced water remediation technologies. We have thoroughly discussed the proposed adsorption mechanism, emphasizing the interaction between the acidic functional groups of selected anti-inflammatory drugs and the basic amine moieties of the polymer within the GO-pAmOx composite. However, this study is not intended to be exhaustive. Further comprehensive investigations, including molecular dynamics simulations, are ongoing to elucidate the detailed adsorption mechanism. This simulation will capture the dynamic evolution of the interactions, offering quite valuable insights into structural fluctuations and the long-term stability of the developed systems. In addition, future investigations will focus on scaling up the synthesis and conducting in-flow experiments to assess the potential for practical implementation in diverse water treatment scenarios.

ASSOCIATED CONTENT

Supporting Information

The Supporting Information is available free of charge at https://pubs.acs.org/doi/10.1021/acsomega.5c00043.

Detailed experimental procedures, ^{1}H NMR spectra of monomer and polymer, UV−vis spectrum of GO, TGA, and ATR(FTIR) of GO-pAmOx after reuse cycles, and calibration curves of all pharmaceuticals (PDF)

AUTHOR INFORMATION

Corresponding Authors

Luca Stefanuto − *Science Department, University of Roma Tre, Rome 00146, Italy*; Email: luca.stefanuto@uniroma3.it

Tecla Gasperi − *Science Department, University of Roma Tre, Rome 00146, Italy; Laboratory of Nanomaterials for Environment and Health (NAMES), Biostructures and Biosystems National Institute (INBB), Rome 00165, Italy*; orcid.org/0000-0003-3638-2517; Email: tecla.gasperi@uniroma3.it

Authors

Agnese Ricci − *Science Department, University of Roma Tre, Rome 00146, Italy*

Elisa Fardelli − *Science Department, University of Roma Tre, Rome 00146, Italy*; orcid.org/0000-0002-4181-1841

Sara Del Galdo − *Science Department, University of Roma Tre, Rome 00146, Italy; Laboratory of Nanomaterials for Environment and Health (NAMES), Biostructures and Biosystems National Institute (INBB), Rome 00165, Italy*

Simone Pepi − *Department of Biotechnology, Chemistry, and Pharmacy, University of Siena, Siena 53100, Italy*

Valerio Graziani − *Science Department, University of Roma Tre, Rome 00146, Italy*

Luca Tortora − *Science Department, University of Roma Tre, Rome 00146, Italy; National Institute of Nuclear Physics (INFN), Roma Tre section, Rome 00185, Italy*; orcid.org/0000-0003-3053-2406

Claudio Rossi − *Department of Biotechnology, Chemistry, and Pharmacy, University of Siena, Siena 53100, Italy*

Valentina Arena − *Microelectronics and Microsystems Institute (IMM) of National Research Council (CNR), Catania 95121, Italy*; orcid.org/0000-0002-7010-9410

Corrado Bongiorno − *Microelectronics and Microsystems Institute (IMM) of National Research Council (CNR), Catania 95121, Italy*

Emanuele Smecca − *Microelectronics and Microsystems Institute (IMM) of National Research Council (CNR), Catania 95121, Italy*; orcid.org/0000-0002-8946-8640

Giovanni Capellini − *Science Department, University of Roma Tre, Rome 00146, Italy*; orcid.org/0000-0002-5169-2823

Barbara Capone − *Science Department, University of Roma Tre, Rome 00146, Italy; Laboratory of Nanomaterials for Environment and Health (NAMES), Biostructures and Biosystems National Institute (INBB), Rome 00165, Italy;* orcid.org/0000-0003-0805-6239

Daniela Tofani − *Science Department, University of Roma Tre, Rome 00146, Italy;* orcid.org/0000-0003-1028-9832

Complete contact information is available at: https://pubs.acs.org/10.1021/acsomega.5c00043

Notes

The authors declare no competing financial interest.

■ ACKNOWLEDGMENTS

The authors wish to thank Saluber Italia s.r.l. and Regione Lazio "Intervento per il rafforzamento della ricerca e innovazione nel Lazio-incentivi per i dottorati di innovazione per le imprese e per la PA"—(ID del Progetto 26084) for supporting this work. This research was also funded by the Grant Excellence Departments 2023−2027 (Department of Science, Roma Tre University), MIUR (articolo 1, commi 314-337 legge 232/2016), Rome Technopole Project (CUP: F83B22000040006 Spoke 6), Contribution from the Bank of Italy (Contributi liberali—Prot. N. 2201555/23 del 21/12/2023), and the financial support from European Union - Next Generation EU (MUR-PRIN2022 PRIN 2022RYP9YT SCOPE CUP:F53D23001130006).

■ REFERENCES

(1) Samal, K.; Mahapatra, S.; Ali, M. H. Pharmaceutical Wastewater as Emerging Contaminants (EC): Treatment Technologies, Impact on Environment and Human Health. *Energy Nexus* **2022**, *6*, No. 100076.

(2) Karpińska, J.; Kotowska, U. Removal of Organic Pollution in the Water Environment. *Water* **2019**, *11*, No. 2017.

(3) Barnes, K. K.; Kolpin, D. W.; Furlong, E. T.; Zaugg, S. D.; Meyer, M. T.; Barber, L. B. A National Reconnaissance of Pharmaceuticals and Other Organic Wastewater Contaminants in the United States — I) Groundwater. *Sci. Total Environ.* **2008**, *402*, 192−200.

(4) Benotti, M. J.; Trenholm, R. A.; Vanderford, B. J.; Holady, J. C.; Stanford, B. D.; Snyder, S. A. Pharmaceuticals and Endocrine Disrupting Compounds in U.S. Drinking Water. *Environ. Sci. Technol.* **2009**, *43*, 597−603.

(5) Loos, R.; Locoro, G.; Comero, S.; Contini, S.; Schwesig, D.; Werres, F.; Balsaa, P.; Gans, O.; Weiss, S.; Blaha, L.; Bolchi, M.; Gawlik, B. M. Pan-European Survey on the Occurrence of Selected Polar Organic Persistent Pollutants in Ground Water. *Water Res.* **2010**, *44*, 4115−4126.

(6) Quesada, H. B.; Baptista, A. T. A.; Cusioli, L. F.; Seibert, D.; De Oliveira Bezerra, C.; Bergamasco, R. Surface Water Pollution by Pharmaceuticals and an Alternative of Removal by Low-Cost Adsorbents: A Review. *Chemosphere* **2019**, *222*, 766−780.

(7) Schaider, L. A.; Rodgers, K. M.; Rudel, R. A. Review of Organic Wastewater Compound Concentrations and Removal in Onsite Wastewater Treatment Systems. *Environ. Sci. Technol.* **2017**, *51* (13), 7304−7317.

(8) Chopra, S.; Kumar, D. Ibuprofen as an Emerging Organic Contaminant in Environment, Distribution and Remediation. *Heliyon* **2020**, *6*, No. e04087.

(9) O'Flynn, D.; Lawler, J.; Yusuf, A.; Parle-McDermott, A.; Harold, D.; McCloughlin, T.; Holland, L.; Regan, F.; White, B. A Review of Pharmaceutical Occurrence and Pathways in the Aquatic Environment in the Context of a Changing Climate and the COVID-19 Pandemic. *Anal. Methods* **2021**, *13*, 575−594.

(10) Ebele, A. J.; Abdallah, M. A.-E.; Harrad, S. Pharmaceuticals and Personal Care Products (PPCPs) in the Freshwater Aquatic Environment. *Emerging Contam.* **2017**, *3*, 1−16.

(11) Kyzas, G. Z.; Fu, J.; Lazaridis, N. K.; Bikiaris, D. N.; Matis, K. A. New Approaches on the Removal of Pharmaceuticals from Wastewaters with Adsorbent Materials. *J. Mol. Liq.* **2015**, *209*, 87−93.

(12) Fernandes, J. P.; Almeida, C. M. R.; Pereira, A. C.; Ribeiro, I. L.; Reis, I.; Carvalho, P.; Basto, M. C. P.; Mucha, A. P. Microbial Community Dynamics Associated with Veterinary Antibiotics Removal in Constructed Wetlands Microcosms. *Bioresour. Technol.* **2015**, *182*, 26−33.

(13) Praveenkumarreddy, Y.; Vimalkumar, K.; Ramaswamy, B. R.; Kumar, V.; Singhal, R. K.; Basu, H.; Gopal, C. M.; Vandana, K. E.; Bhat, K.; Udayashankar, H. N.; Balakrishna, K. Assessment of Non-Steroidal Anti-Inflammatory Drugs from Selected Wastewater Treatment Plants of Southwestern India. *Emerging Contam.* **2021**, *7*, 43−51.

(14) Singh, N. B.; Nagpal, G.; Agrawal, S.; Rachna. Water Purification by Using Adsorbents: A Review. *Environ. Technol. Innovation* **2018**, *11*, 187−240.

(15) Ramazani, A.; Oveisi, M.; Sheikhi, M.; Gouranlou, F. Natural Polymers as Environmental Friendly Adsorbents for Organic Pollutants Such as Dyes Removal from Colored Wastewater. *Curr. Org. Chem.* **2018**, *22*, 1297−1306.

(16) Mahand, S. N.; Aliakbarzadeh, S.; Moghaddam, A.; Moghaddam, A. S.; Kruppke, B.; Nasrollahzadeh, M.; Khonakdar, H. A. Polyoxazoline: A Review Article from Polymerization to Smart Behaviors and Biomedical Applications. *Eur. Polym. J.* **2022**, *178*, No. 111484.

(17) Kanazaki, K.; Sano, K.; Makino, A.; Homma, T.; Ono, M.; Saji, H. Polyoxazoline Multivalently Conjugated with Indocyanine Green for Sensitive in Vivo Photoacoustic Imaging of Tumors. *Sci. Rep.* **2016**, *6*, No. 33798.

(18) Lorson, T.; Lübtow, M. M.; Wegener, E.; Haider, M. S.; Borova, S.; Nahm, D.; Jordan, R.; Sokolski-Papkov, M.; Kabanov, A. V.; Luxenhofer, R. Poly(2-Oxazoline)s Based Biomaterials: A Comprehensive and Critical Update. *Biomaterials* **2018**, *178*, 204−280.

(19) Hoogenboom, R. Poly(2-Oxazoline)s: A Polymer Class with Numerous Potential Applications. *Angew. Chem., Int. Ed.* **2009**, *48*, 7978−7994.

(20) Bauer, M.; Lautenschlaeger, C.; Kempe, K.; Tauhardt, L.; Schubert, U. S.; Fischer, D. Poly(2-ethyl-2-oxazoline) as Alternative for the Stealth Polymer Poly(Ethylene Glycol): Comparison of in Vitro Cytotoxicity and Hemocompatibility. *Macromol. Biosci.* **2012**, *12*, 986−998.

(21) Schlaad, H.; Diehl, C.; Gress, A.; Meyer, M.; Demirel, A. L.; Nur, Y.; Bertin, A. Poly(2-oxazoline)s as Smart Bioinspired Polymers. *Macromol. Rapid Commun.* **2010**, *31*, 511−525.

(22) Roma, E.; Corsi, P.; Willinger, M.; Leitner, N. S.; Zirbs, R.; Reimhult, E.; Capone, B.; Gasperi, T. Theoretical and Experimental Design of Heavy Metal-Mopping Magnetic Nanoparticles. *ACS Appl. Mater. Interfaces* **2021**, *13*, 1386−1397.

(23) Stefanuto, L.; Ricci, A.; Del Galdo, S.; Rossi, C.; Pepi, S.; Giordano, E.; Capone, B.; Tofani, D.; Gasperi, T. 2-Oxazoline-Based Polymer for Pharmaceutical Products Adsorption in Aqueous Media. *J. Polym. Sci.* **2024**, *62*, 5656−5664.

(24) Ricci, A.; Stefanuto, L.; Del Galdo, S.; Fardelli, E.; Pepi, S.; Casciardi, S.; Capone, B.; Rossi, C.; Tofani, D.; Capellini, G.; Iucci, G.; Masci, G.; Gasperi, T. Molecularly Imprinted Poly(2-(3-(Amino)Propyl)-2-Oxazoline) for the Selective Removal of Ibuprofen from Aqueous Solutions. *ACS Appl. Polym. Mater.* **2025**, *7*, 42−53.

(25) Dreyer, D. R.; Park, S.; Bielawski, C. W.; Ruoff, R. S. The Chemistry of Graphene Oxide. *Chem. Soc. Rev.* **2010**, *39*, 228−240.

(26) Thakur, K.; Kandasubramanian, B. Graphene and Graphene Oxide-Based Composites for Removal of Organic Pollutants: A Review. *J. Chem. Eng. Data* **2019**, *64*, 833−867.

(27) Kozur, A.; Burk, L.; Thomann, R.; Lutz, P. J.; Mülhaupt, R. Graphene Oxide Grafted with Polyoxazoline as Thermoresponsive Support for Facile Catalyst Recycling by Reversible Thermal Switching between Dispersion and Sedimentation. *Polymer* **2019**, *178*, No. 121553.
(28) Petrović, S.; Savić, S.; Zvezdanović, J.; Nikolić, L.; Stojiljković, S. Benzoic Acid Removal from Aqueous Solutions by Activated Charcoal. *Adv. Technol.* **2021**, *10*, 5−10.
(29) Shahriary, L.; Athawale, A. Graphene Oxide Synthesized by Using Modified Hummers Approach. *Int. J. Renewable Energy Environ. Eng.* **2014**, *2*, 58−63.
(30) Xue, Y.; Liu, Y.; Lu, F.; Qu, J.; Chen, H.; Dai, L. Functionalization of Graphene Oxide with Polyhedral Oligomeric Silsesquioxane (POSS) for Multifunctional Applications. *J. Phys. Chem. Lett.* **2012**, *3*, 1607−1612.
(31) Ohno, K.; Zhao, C.; Nishina, Y. Polymer-Brush-Decorated Graphene Oxide: Precision Synthesis and Liquid-Crystal Formation. *Langmuir* **2019**, *35*, 10900−10909.
(32) Wang, J. Functionalization of Graphene Oxide with Polysilicone: Synthesis, Characterization, and Its Flame Retardancy in Epoxy Resin. *Polymers* **2021**, *13*, No. 3857.
(33) Chung, H.-K.; Kim, W.-H.; Park, J.; Cho, J.; Jeong, T.-Y.; Park, P.-K. Application of Langmuir and Freundlich Isotherms to Predict Adsorbate Removal Efficiency or Required Amount of Adsorbent. *J. Ind. Eng. Chem.* **2015**, *28*, 241−246.
(34) Lesmana, S. O.; Febriana, N.; Soetaredjo, F. E.; Sunarso, J.; Ismadji, S. Studies on Potential Applications of Biomass for the Separation of Heavy Metals from Water and Wastewater. *Biochem. Eng. J.* **2009**, *44*, 19−41.
(35) Ndoun, M. C.; Elliott, H. A.; Preisendanz, H. E.; Williams, C. F.; Knopf, A.; Watson, J. E. Adsorption of Pharmaceuticals from Aqueous Solutions Using Biochar Derived from Cotton Gin Waste and Guayule Bagasse. *Biochar* **2021**, *3*, 89−104.
(36) Alcalde-Garcia, F.; Prasher, S.; Kaliaguine, S.; Tavares, J. R.; Dumont, M.-J. Desorption Strategies and Reusability of Biopolymeric Adsorbents and Semisynthetic Derivatives in Hydrogel and Hydrogel Composites Used in Adsorption Processes. *ACS Eng. Au* **2023**, *3*, 443−460.
(37) Schroffenegger, M.; Reimhult, E. Thermoresponsive Core-Shell Nanoparticles: Does Core Size Matter? *Materials* **2018**, *11* (9), No. 1654.
(38) Madikizela, L. M.; Zunngu, S. S.; Mlunguza, N. Y.; Tavengwa, N. T.; Mdluli, P. S.; Chimuka, L. Application of Molecularly Imprinted Polymer Designed for the Selective Extraction of Ketoprofen from Wastewater. *Water SA* **2018**, *44* (3), 406−418, DOI: 10.4314/wsa.v44i3.08.
(39) Bui, T. X.; Choi, H. Adsorptive Removal of Selected Pharmaceuticals by Mesoporous Silica SBA-15. *J. Hazard. Mater.* **2009**, *168*, 602−608.

https://doi.org/10.1021/acsomega.5c00043
ACS Omega 2025, 10, 30087−30099